ACS APPLIED MATERIALS & INTERFACES

Letter

www.acsami.org

Porous Inorganic Materials from Living Porogens: Channel-like TiO_2 from Yeast-Assisted Sol–Gel Process

Yi-Chun Chang,[†] Chi-Young Lee,[‡] and Hsin-Tien Chiu*[,†]

[†]Department of Applied Chemistry, National Chiao Tung University, Hsinchu, Taiwan 30010, R. O. C.

[‡]Department of Materials Science and Engineering, National Tsing Hua University, Hsinchu, Taiwan 30013, R. O. C.

Supporting Information

ABSTRACT: Vitality of yeast cells maintained in an aqueous sol–gel solution containing titanium tetraisopropoxide and glucose. The living cells and their metabolites acted as the porogens for a channel-like TiO_2 precursor. Further processing of the precursor offered a channel-like meso/macroporous TiO_2, a potential anode material for Li-ion battery.

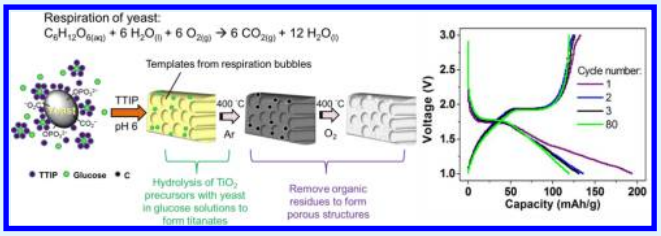

KEYWORDS: *biosynthesis, sol–gel processes, mesoporous materials, titanium dioxide, lithium-ion battery*

INTRODUCTION

Biological materials display natural structures that are difficult to obtain through artificial synthetic ways. Recently, the use of organisms as templates for the generation of unique inorganic structures and materials has received increasing attention.[1,2] It would be interesting to observe the behavior of "living" cells in a synthetic environment leading to the fabrication of artificial materials.[3,4] The term biocers (biologically modified ceramics) is a class of nanocomposites that combines biocomponents with ceramic-like matrices.[5] Biocomponents are usually prokaryotes (bacteria and fungi),[6,7] eukaryotes (animal and plant cells),[8−10] and cell-derived subunits (protein, enzymes, and DNA).[11,12] Nonetheless, in most of these cases, physiological activities of the bio-components were not maintained. They only act as lifeless templates to assist the formation of specific morphology and shapes. In nature, shells and corals are usually composed of $CaCO_3$ secreted by the organisms. The blood of mollusca contains minerals that are the source of the shell. $CaCO_3$ is not only the metabolite but also the major composition of bones of coral. By such characteristics, ureolytic bacteria are able to precipitate $CaCO_3$ in their environment by converting urea into NH_3 and CO_3^{2-}. The process could be applied for repairing cracks in concretes.[13] Therefore, organisms might maintain their viability in mild environments in principle.

Yeast (*Saccharomyces cerevisiae*) is one of the most popular eukaryotic micro-organism in molecular and cell biology. Its external structure and functional organization are similar to the cells of high-level organisms. Its solid cell wall and negatively charged surface have been applied as sacrificial templates for the formation of porous inorganic-structures.[14,15] Yeasts are popular porogens because they not only provide hard cell walls but also generate gaseous metabolites. Because yeast has a short generation time, it could be easily incubated. Bread is a product of the yeast metabolism. On the other hand, cases involving the formation of porous inorganic structures from living porogens are rare. The only one reported in literature briefly discussed the synthesis of porous silica via a sol–gel route in the presence of yeast.[16] In this study, we employed a simple sol–gel process to fabricate TiO_2 precursors by reacting titanium tetraisopropoxide (TTIP, $Ti(O^iPr)_4$), instant yeast, and glucose in an aqueous solution. Remarkably, the yeast cells maintained their physiological activities while TTIP molecules polymerized into a low toxicity titanate precursor. It is known that the toxicity of TiO_2 towards yeast is much less than other metal oxides, such as ZnO and CuO.[17,18] After further processing, porous channel-like TiO_2 was prepared. In addition, potential applications of the as-prepared TiO_2 in Li ion batteries were explored. Our preliminary results are reported below.

RESULTS AND DISCUSSION

In a typical experiment, instant yeast supplied locally was added to an aqueous solution containing glucose and TTIP at room temperature. The yeast cells were alive in the aerobic reaction mixture for several hours. Figure 1 shows a series of time-lapse images of yeast in an aqueous mixture of glucose and TTIP. Bubbles were formed in the mixture. After 15 min, its volume expanded significantly (Figure 1b). Clearly, this was the physiological phenomenon of the yeast cells. The mixture remained bubbling and expanded further after 30 min (Figure 1c). After 45 min (Figure 1d), the volume increased six-fold while the acidity of the mixture increased slightly to pH 5−6. The time-lapse images reveal that the swelling phenomenon is analogous to the leavening process of dough in bakeries. Apparently, even in the presence of TTIP and its hydrolysis/

Received: November 15, 2013
Accepted: December 16, 2013
Published: December 16, 2013

   dx.doi.org/10.1021/am405149a | ACS Appl. Mater. Interfaces 2014, 6, 31−35

Figure 1. Time-lapse images of the mixture of TTIP and aqueous glucose solution in the presence of yeast. (a) 0, (b) 15, (c) 30, and (d) 45 min. The original images are shown in Figure S1 in the Supporting Information.

condensation products, the glucose metabolism in the yeast cells was maintained for about 90 min. Their respirations produced CO_2 and H_2O as the metabolites. Without glucose, an aqueous mixture of yeast and TTIP did not show any obvious volume variation (Figure S2 in the Supporting Information).

Because of the presence of a thick sol–gel matrix, many methods for monitoring living yeast are impractical in our case.[19−23] Instead, optical microscopic images of the yeast cells in an aqueous solution of glucose and TTIP were taken. In Figure 2a, the growth of a bud on a parent cell is observed. Similar cases are found frequently in Figure S3 in the Supporting Information. As displayed in Figure 2b, some yeast cells are covered by layers of inorganic solids, the sol–gel intermediates formed by the condensation of TTIP molecules. The budding phenomenon is the result of common asexual reproductive mode of *Saccharomyces cerevisiae*. This observation suggests that the yeast cells not only respire but also reproduce in the presence of TTIP and its hydrolysis/condensation products for several hours. According to the physiology of yeast, the life cycle passes through the initial lag phase defined as a short adaptation stage. And then, the cells are metabolically active through a few reproductions. Thus, the overall cell population increases in the exponential phase, reaches the steady phase, and finally decreases in the decline phase. In our study, the presence of TTIP indeed caused premature decline of the yeast population, as the bubbling phenomenon ceased after ca. 2 h. Another reason for the gradual cell deaths is attributed to the consumption of glucose in the process.

As discussed above, we envision that both the CO_2 bubbles from the yeast respiration and the physical cell structures can act cooperatively as the "living templates" to assist the formation of a porous TiO_2 precursor. The light-yellow "inorganic dough" isolated from the reaction suspension was dried. The SEM image in Figure S4 in the Supporting Information reveals its porous nature. The solid was annealed in Ar, and then, oxidized in O_2 atmosphere to remove all organic residues. After the processing, a white solid was isolated in nearly quantitative yield. Its bulk density was 0.29 g/cm^3, much lower than the value of commercial bulk TiO_2, 0.7−0.9 g/cm^3. The observation is consistent with the porous nature of the solid. The total pore volume is estimated to be ca. 65 % of the total volume. The scanning electron microscopic (SEM) images in Figure 3 depict the porous nature of the product. They display numerous mesopores with diameters tens of nm (Figure 3a, b) and straight channels with diameters ca. 1 μm and lengths ca. 10 μm (Figure 3a, c, d). The channel-like morphology differs from the results that employed yeast cells as the sacrificial templates.[7,14] In these cases, the porous products obtained their morphology from the deceased yeast cells. In this study, we attribute the channel formation to the bubbling action of CO_2 generated by the cell respiration. A high resolution transmission electron microscopic (HRTEM) image in Figure S5 in the Supporting Information and a powder X-ray diffraction (XRD) pattern in Figure S6 in the Supporting Information confirm that the solid product was composed of anatase (major) and rutile (minor) TiO_2.

By using N_2 adsorption-desorption analyses (see Figure S7a in the Supporting Information), a specific surface area 63 m^2/g is estimated for the solid using the Brunauer–Emmett–Teller (BET) equation. The type IV hysteresis loop of the isotherm reveals some capillary condensation behavior at relatively high pressures. The pore size distribution (see Figure S7b in the Supporting Information) from the Barrett–Joyner–Halenda (BJH) method suggests the presence of smaller (diameter 3.7 nm, with a distribution 2−10 nm) and lager (diameter 40 nm, with a distribution 10−100 nm) mesopores. These are comparable to the pores observed in Figure 3b. As a result, the proportion of the volume occupied by the mesopores is 37%, whereas that occupied by the macropores is 63% of the total volume of all pores. The amount of yeast added into the solution affected the specific surface areas of the porous products (Figure 4). Without yeast, the product shows a specific surface area 34 m^2/g. As the amount of yeast added increases, the BET surface area is increased as well. For the sample used 2.5 g of yeast, a specific area 63 m^2/g is observed. Therefore, we discover a tendency that each additional gram of

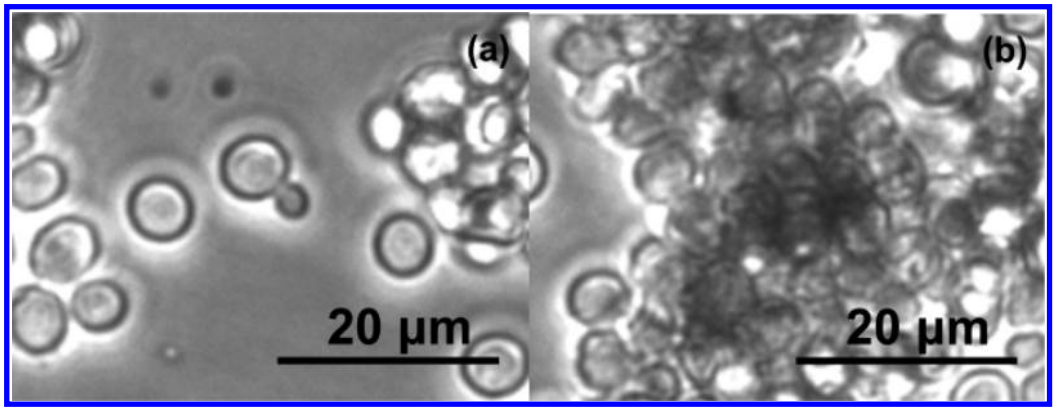

Figure 2. Optical images of yeast cells in an aqueous solution of glucose and TTIP. (a) Bud on a yeast cell. (b) Yeast cells covered by condensed inorganic solids. The images are taken from the photograph shown in Figure S3 in the Supporting Information.

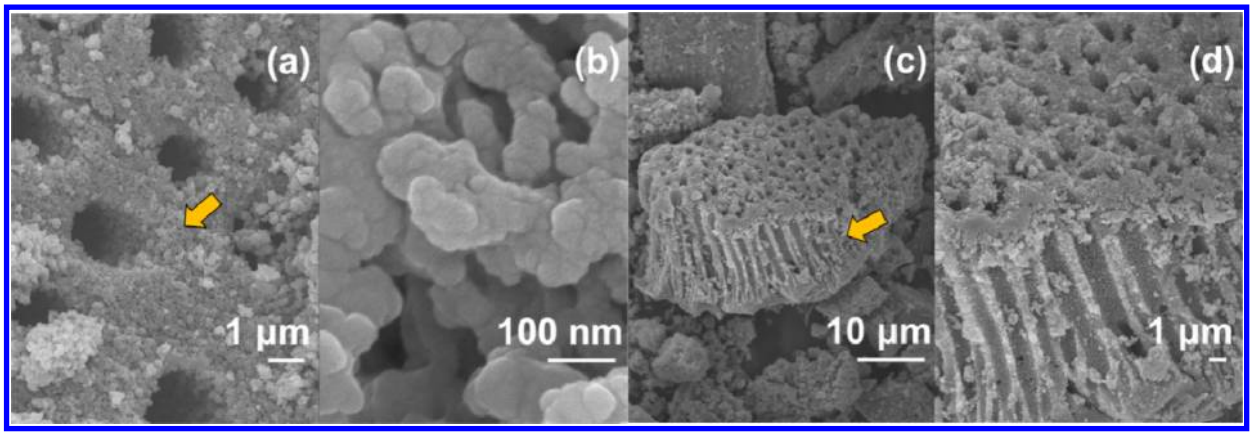

Figure 3. SEM images. (a) Top-view. (b) Enlarged view from the marked area in a. (c) Side-view image. (d) Enlarged view from the marked area in c.

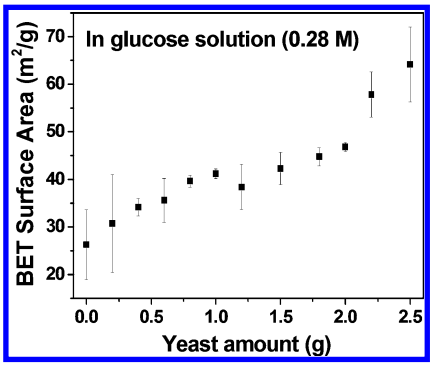

Figure 4. Effect of the amount of yeast on the BET surface areas of the porous materials.

yeast would increase an area ca. 6 m^2. In contrast, a porous TiO_2 sample prepared without the addition of yeast and glucose showed a specific surface area 80 m^2/g. We suggest that in the reaction without any glucose and yeast, TTIP molecules undergo condensation freely to form a low density sol–gel precursor. This would lead to the high surface area product. When glucose is added, TTIP would react with the hydroxyl groups of the monosaccharide and use it as the center for the condensation polymerization.[24] Thus, the product is denser with a much smaller surface area. When both glucose and yeast are added to the solution containing TTIP, gaseous CO_2 is generated by the metabolism of glucose in the cells. The bubbling action may generate less dense sol–gel precursors that provide higher-surface-area porous TiO_2 products.[16] One of the factors that affects the growth and respiration activities of yeast is temperature. Generally, temperatures suitable for the metabolism of baker's yeast are 25–30 °C. Below the temperature range, the activity of yeast increases as the temperature is raised. Nonetheless, the temperature above the desirable range is harmful for the yeast growth. Consequently, although the channel morphology still exists for the samples incubated at 35 and 50 °C (see Figure S8 in the Supporting Information), their final specific surface areas are reduced to 45 and 40 m^2/g, respectively.

A reaction pathway is proposed in Scheme 1 to rationalize the formation of the channel-like porous TiO_2. Glucose molecules can function both as the center for the hydrolysis/condensation polymerization of TTIP and as the nutrient for yeast. The cells maintain physiological activities while their respiration generates CO_2 bubbles. The as-formed carbonic acid lowers the pH of the mixture. Gradually, layers of titanates mixed with unconsumed glucose molecules accumulate on cell surfaces while the evolution of CO_2 produces numerous channels in the inorganic matrix. The bubbling action, the cells, and the residual glucose molecules act together as the pore generation templates. Similar hypothesis for pore generation through the bubbling effect has been proposed recently.[25] After the inorganic/organic mixture is processed further at 400 °C under Ar, the deceased cells, the unreacted molecules, and the

Scheme 1. Proposed Pathway for the Formation of Channel-like Porous TiO_2

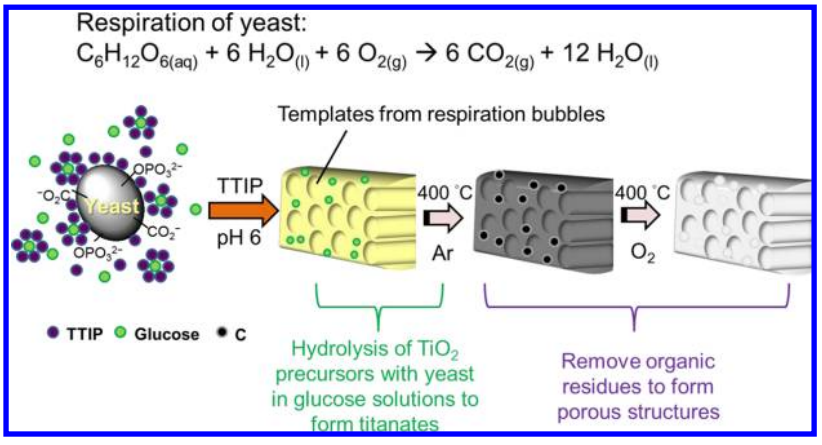

dx.doi.org/10.1021/am405149a | ACS Appl. Mater. Interfaces 2014, 6, 31–35

residual isopropoxy ligands are either vaporized to leave empty spaces or decomposed into nanosized carbon particles. At 400 °C in O_2, all carbon residues are oxidized to offer mesopores, whereas the titanate crystallizes into the channel-like porous TiO_2.

Li-ion batteries are one of the major electrical power storage devices.[26,27] Intercalation of Li^+ ions into TiO_2 displays a small volume change (<4%). This differs from other common anode materials, graphite, Si, and Sn.[28−30] Their high volume changes (10−400%) during charge/discharge cycling induce irreversible structural destruction. The small TiO_2 lattice variation during Li^+ intercalation/deintercalation maintains its structural stability and cycle life.[31−35] During the discharging, Li^+ ions intercalate into the octahedral sites of anatase TiO_2 and convert it to Li_xTiO_2 ($x \approx 0.5$) by the following electrochemical process, eq 1, in a TiO_2/Li half-cell[36,37]

$$TiO_2 + xLi^+ + xe^- \rightarrow Li_xTiO_2 \quad (1)$$

In this study, we explored the possibility of using the channel-like porous TiO_2 as the cathode in half-cell type coin cells (CR2032). A piece of Li metal was used as the anode in the assembled device. The first discharge−charge cycle shows an irreversible capacity loss (31% at 0.1 *C*) in Figure 5a. This agrees with the literature data (30−50 %).[38,39] The battery maintains a reversible capacity 136 mAh/g at the discharge rate 0.1 *C*. After cycled at various discharge/charge rates 80 times, the device still retains a respectable capacity 120 mAh/g (Figure 5b). For comparison, performances of samples prepared without the presence of glucose, yeast, or both are also represented in Figure 5b. All of the samples do not show channel morphology (see Figure S9a in the Supporting Information). Their specific surface areas are 50 m^2/g (without glucose, addition of 2.5 g of yeast), 34 m^2/g (without yeast, addition of 0.5 g of glucose), and 80 m^2/g (without glucose and yeast). Most of them are composed of anatase phase TiO_2 (see Figure S9b in the Supporting Information). Performances of the cathodes fabricated from those samples reveal lower capacities than the sample synthesized in the presence of living yeast cells, especially at high discharge rates. There are several possible reasons for the differences. Because all of them do not have channel structures (due to the lack of physiological activity), the intercalation/deintercalation of Li^+ ions in them may not be as fast as in the channel-like porous TiO_2 prepared in this study. The sample prepared without the addition of yeast shows the worst performance. Probably, glucose molecules function as the center for the hydrolysis/condensation polymerization of TTIP. Thus, the as-prepared sample has the smallest specific surface area. The observations do suggest that the unique porous structure of the TiO_2 prepared from the living porogen route probably provides easily accessible sites for the intercalation/deintercalation of Li^+ ions in the batteries. This is also comparable to recent observations employing electrodes composed of meso/macro-porous TiO_2 synthesized using different strategies.[25,40] On the basis of the preliminary observations reported here, we anticipate that the performance of our unique TiO_2 structure can be improved further.

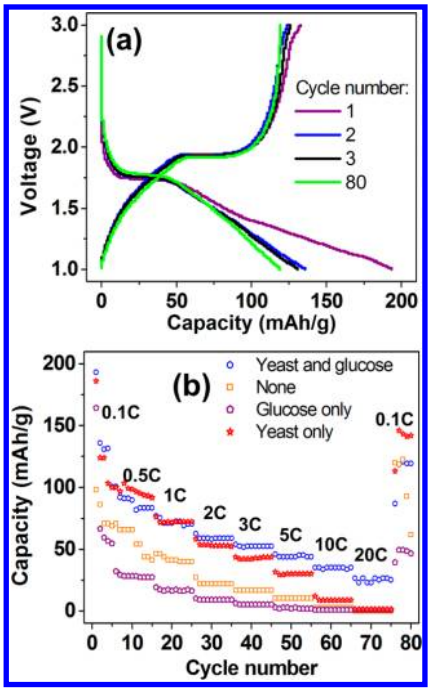

Figure 5. (a) Profiles of the first discharge/charge (0.1 *C*) cycles of Li-ion battery fabricated from the channel-like porous TiO_2. (b) Performance of Li-ion batteries at different discharge rates for 80 cycles (1 *C* = 334 mAh/g; yeast and glucose, sample prepared in the presence of yeast and glucose; none, sample prepared without the addition of yeast and glucose; glucose only, only glucose was added; yeast only, only yeast was added).

CONCLUSIONS

In summary, instant yeast cells maintain their physiological activities for several hours in an aqueous glucose solution containing TTIP. As TTIP polymerizes via a sol−gel route on the cells, bubbles of CO_2 from the cell respiration generate numerous channels in the precursor. Glucose and yeast work cooperatively to offer the final meso/macro porous channel-like structure. The as-formed porous TiO_2 can function as an electrode material for Li-ion battery. These unique hierarchically-structured porous materials may find potential applications in other areas.[41] By controlling the physiological environment for yeast growth and using different alkoxides, other metal oxides with unique properties could be obtained.

ASSOCIATED CONTENT

Supporting Information

Experimental section, time lapse images, optical micrograph, XRD pattern, specific surface area data, and SEM and HRTEM images. This material is available free of charge via the Internet at http://pubs.acs.org.

AUTHOR INFORMATION

Corresponding Author

*E-mail: htchiu@nctu.edu.tw.

Notes

The authors declare no competing financial interest.

ACKNOWLEDGMENTS

We thank Industrial Technology Research Institute of Taiwan, R.O.C, for assembly of the battery and the National Science Council, "Aim for the Top University Plan" of the National Chiao Tung University, and the Ministry of Education of Taiwan, the Republic of China.

REFERENCES

(1) Studart, A. R.; Gonzenbach, U. T.; Tervoort, E.; Gauckler, L. J. *J. Am. Ceram. Soc.* **2006**, *89*, 1771−1789.
(2) van Bommel, K. J. C.; Friggeri, A.; Shinkai, S. *Angew. Chem., Int. Ed.* **2003**, *42*, 980−999.
(3) Blondeau, M.; Coradin, T. *J. Mater. Chem.* **2012**, *22*, 22335−22343.
(4) Godlewska-Żyłkiewicz, B. *Anal. Bioanal. Chem.* **2006**, *384*, 114−123.
(5) Bottcher, H.; Soltmann, U.; Mertig, M.; Pompe, W. *J. Mater. Chem.* **2004**, *14*, 2176−2188.
(6) Nomura, T.; Morimoto, Y.; Tokumoto, H.; Konishi, Y. *Mater. Lett.* **2008**, *62*, 3727−3729.
(7) Bai, B.; Wang, P.; Wu, L.; Yang, L.; Chen, Z. *Mater. Chem. Phys.* **2009**, *114*, 26−29.
(8) Schnepp, Z.; Yang, W.; Antonietti, M.; Giordano, C. *Angew. Chem., Int. Ed.* **2010**, *49*, 6564−6566.
(9) Shi, N.; Li, X.; Fan, T.; Zhou, H.; Ding, J.; Zhang, D.; Zhu, H. *Energy Environ. Sci.* **2011**, *4*, 172−180.
(10) Yang, D.; Fan, T.; Zhang, D.; Zhu, J.; Wang, Y.; Du, B.; Yan, Y. *Chem.—Eur. J.* **2013**, *19*, 4742−4747.
(11) Yan, J.; Wu, G.; Li, L.; Yu, A.; Sun, X.; Guan, N. *J. Nanosci. Nanotechnol.* **2010**, *10*, 5767−5775.
(12) Numata, M.; Sugiyasu, K.; Hasegawa, T.; Shinkai, S. *Angew. Chem., Int. Ed.* **2004**, *43*, 3279−3283.
(13) Van Tittelboom, K.; De Belie, N.; De Muynck, W.; Verstraete, W. *Cem. Concr. Res.* **2010**, *40*, 157−166.
(14) Chia, S.; Urano, J.; Tamanoi, F.; Dunn, B.; Zink, J. I. *J. Am. Chem. Soc.* **2000**, *122*, 6488−6489.
(15) He, W.; Cui, J.; Yue, Y.; Zhang, X.; Xia, X.; Liu, H.; Lui, S. *J. Colloid Interface Sci.* **2011**, *354*, 109−115.
(16) Manap, N. R. A.; Jais, U. S. *Mater. Res. Innovations* **2009**, *13*, 382−385.
(17) Huang, Y.-W.; Wu, C.-h.; Aronstam, R. S. *Materials* **2010**, *3*, 4842−4859.
(18) Kasemets, K.; Ivask, A.; Dubourguier, H.-C.; Kahru, A. *Toxicol. In Vitro* **2009**, *23*, 1116−1122.
(19) Sagot, I.; Bonneu, M.; Balguerie, A.; Aigle, M. *FEBS Lett.* **1999**, *447*, 53−57.
(20) Hediger, F.; Taddei, A.; Neumann, F. R.; Gasser, S. M. In *Methods in Enzymology*; Allis, C. D., Carl, W., Eds.; Academic Press: New York, 2003; Vol. Vol. 375, p 345−365.
(21) Wang, B.; Liu, P.; Jiang, W.; Pan, H.; Xu, X.; Tang, R. *Angew. Chem., Int. Ed.* **2008**, *47*, 3560−3564.
(22) Fraser, C. G. *J. Phys. Chem.* **1919**, *24*, 741−748.
(23) Bonora, A.; Mares, D. *Curr. Microbiol.* **1982**, *7*, 217−221.
(24) Yang, D.-H.; Takahara, N.; Lee, S.-W.; Kunitake, T. *Sens. Actuators, B* **2008**, *130*, 379−385.
(25) Wang, H.; Yang, H.; Lu, L.; Zhou, Y.; Wang, Y. *Dalton Trans.* **2013**, *42*, 8781−8787.
(26) Liu, D.; Cao, G. *Energy Environ. Sci.* **2010**, *3*, 1218−1237.
(27) Zhang, X.; He, W.; Yue, Y.; Wang, R.; Shen, J.; Liu, S.; Ma, J.; Li, M.; Xu, F. *J. Mater. Chem.* **2012**, *22*, 19948−19956.
(28) Yang, Z.; Choi, D.; Kerisit, S.; Rosso, K. M.; Wang, D.; Zhang, J.; Graff, G.; Liu, J. *J. Power Sources* **2009**, *192*, 588−598.
(29) Hsu, K.-C.; Liu, C.-E.; Chen, P.-C.; Lee, C.-Y.; Chiu, H.-T. *J. Mater. Chem.* **2012**, *22*, 21533−21539.
(30) Lafont, U.; Carta, D.; Mountjoy, G.; Chadwick, A. V.; Kelder, E. M. *J. Phys. Chem. C* **2009**, *114*, 1372−1378.
(31) Zhang, D.; Wen, M.; Zhang, P.; Zhu, J.; Li, G.; Li, H. *Langmuir* **2012**, *28*, 4543−4547.
(32) Kubiak, P.; Fröschl, T.; Hüsing, N.; Hörmann, U.; Kaiser, U.; Schiller, R.; Weiss, C. K.; Landfester, K.; Wohlfahrt-Mehrens, M. *Small* **2011**, *7*, 1690−1696.
(33) Park, K.-S.; Min, K.-M.; Jin, Y.-H.; Seo, S.-D.; Lee, G.-H.; Shim, H.-W.; Kim, D.-W. *J. Mater. Chem.* **2012**, *22*, 15981−15986.
(34) Feckl, J. M.; Fominykh, K.; Döblinger, M.; Fattakhova-Rohlfing, D.; Bein, T. *Angew. Chem., Int. Ed.* **2012**, *51*, 7459−7463.
(35) Chen, P.-C.; Tsai, M.-C.; Chen, H.-C.; Lin, I. N.; Sheu, H.-S.; Lin, Y.-S.; Duh, J.-G.; Chiu, H.-T.; Lee, C.-Y. *J. Mater. Chem.* **2012**, *22*, 5349−5355.
(36) Chen, J. S.; Tan, Y. L.; Li, C. M.; Cheah, Y. L.; Luan, D.; Madhavi, S.; Boey, F. Y. C.; Archer, L. A.; Lou, X. W. *J. Am. Chem. Soc.* **2010**, *132*, 6124−6130.
(37) Wang, Z.; Lou, X. W. *Adv. Mater.* **2012**, *24*, 4124−4129.
(38) Xu, J.; Jia, C.; Cao, B.; Zhang, W. F. *Electrochim. Acta* **2007**, *52*, 8044−8047.
(39) Armstrong, A. R.; Armstrong, G.; Canales, J.; García, R.; Bruce, P. G. *Adv. Mater.* **2005**, *17*, 862−865.
(40) Liu, H.; Bi, Z.; Sun, X.-G.; Unocic, R. R.; Paranthaman, M. P.; Dai, S.; Brown, G. M. *Adv. Mater.* **2011**, *23*, 3450−3454.
(41) Li, Y.; Fu, Z.-Y.; Su, B.-L. *Adv. Funct. Mater.* **2012**, *22*, 4634−4667.